

Long-term effects of biochar amount on the content and composition of organic matter in soil aggregates under field conditions

Xinliang Dong¹ · Tianyu Guan¹ · Guitong Li¹ · Qimei Lin¹ · Xiaorong Zhao¹

Received: 31 August 2015 / Accepted: 12 December 2015 / Published online: 25 January 2016
© Springer-Verlag Berlin Heidelberg 2016

Abstract

Purpose Soil aggregates play an important role in promoting soil fertility, as well as increasing the sink capacity and stability of soil carbon. In this study, we consider the following research questions:

1. Under field conditions, do different dosages of biochar increase the soil aggregation after 3 years of application?
2. How does the application of biochar affect the concentration and distribution of soil total organic carbon (TOC) and total nitrogen (TN) in different sizes of aggregates?
3. Can the application of biochar alter the composition of organic carbon in soil aggregates?

Materials and methods Different amounts of biochar (up to 90 t ha⁻¹) were applied to a calcareous soil in a field experiment in 2009 along with the application of chemical fertilizer annually and the returning of winter wheat and summer maize straws. After 3 years, 0–20-cm soil samples were taken to measure the size distribution of soil water-stable aggregates by wet sieving, the concentrations of TOC and TN in whole aggregates and light or heavy fractions by elemental analysis equipment, and composition of TOC by Fourier transform infrared (FTIR) and pyrolysis-gas chromatography/mass spectrometer (Py–GC/MS).

Results and discussion (1) The 3 years of biochar application had no significant effects on degree of soil aggregation but reduced the breakage of large soil aggregates (>1000 μm); (2) biochar significantly increased the contents of TOC and TN in soil macro-aggregates (>250 μm), as well as their ratios to total soil amount. Biochar also significantly increased the contents of TOC and TN in light fractions as well as the C/N ratio, which made the soil organic matter more active. The biochar dosage showed a significant positive correlation with organic carbon, total nitrogen, and C/N ratio in light fraction components of aggregates (>250 μm). Biochar mainly affected the organic matter in the heavy fraction components of macro-aggregates; (3) from the Py–GC/MS results, biochar increased the CO₂ content originated from active organic carbon.

Conclusions Long-term application of biochar improved the stability of soil aggregates, increased the contents of TOC and TN as well as organic carbon and total nitrogen in macro-aggregates, and usually increased the contents of CO₂ originated from active organic carbon in light fractions. The findings were helpful in evaluating the effects of biochar on soil aggregation and organic matter stability.

Keywords Biochar · C/N · Field experiments · Light-fraction organic carbon · Soil aggregates

Responsible editor: Chengrong Chen

Electronic supplementary material The online version of this article (doi:10.1007/s11368-015-1338-5) contains supplementary material, which is available to authorized users.

✉ Guitong Li
lgtong@cau.edu.cn

¹ College of Resources and Environment, China Agricultural University, Beijing 100193, People's Republic of China

1 Introduction

The formation of soil aggregates has an important role in improving soil water-retaining capacity, reducing cultivation resistance, enhancing soil aeration, and protecting soil organic carbon (SOC), and is generally widely studied. The formation and stability of soil aggregates are affected by many factors, such as soil animals, plant root systems, microorganisms, and soil organic matter content (Six et al. 2004). The soil

aggregates and SOC are interdependent; aggregates protect SOC from decomposition, while SOC assists in aggregate formation (Oades and Waters 1991).

Biochar is a solid material rich in stable organic carbon and is formed by the pyrolysis of organic materials under high temperatures and oxygen-free conditions (Laird et al. 2009). Research has shown that biochar application can reduce soil bulk density, improve soil water-holding capacity (Lu et al. 2014; Peake et al. 2014; Mollinedo et al. 2015), enhance effectiveness of soil cation exchange (Jien and Wang 2013; Chintala et al. 2014a), and improve soil aggregation and stability (Liu et al. 2014; Lu et al. 2014; Soenne et al. 2014). In addition, biochar can enhance soil microorganism activity and indirectly change the mineralization rate of SOC, which in turn influences the formation process of soil aggregates (Steiner et al. 2008). To our knowledge, no consistent conclusions currently exist on the effects of biochar on the numbers and stability of soil aggregates in response to changing biochar species diversity, biochar dosage, or soil conditions (Hardie et al. 2014; Jeffery et al. 2015; Ojeda et al. 2015).

SOC composition is complex with various stabilities and contents in different sizes of aggregates (Six et al. 2004; Liu et al. 2014). The SOC can be classified into light or heavy fractions based on the density variation. The light fraction mainly includes residues and fragments of plants and animals, mycelium, spores, monosaccharide, polysaccharide, hemilignin, and other residues (Christensen 2001). It has strong decomposability and is thus difficult to preserve in soil. The heavy fraction, with humus as its main component, is resistant to decomposition and relatively stable (Christensen 1992). Research has shown that biochar can increase the content of SOC in soil aggregates (Liu et al. 2014); however, its effect on the contents of total organic carbon (TOC) and total nitrogen (TN) in different sizes of aggregates, the TOC and TN in light and heavy fractions, and the composition of the organic carbon remains unclear. The analytical technologies of Fourier transform infrared spectra (FTIR) and pyrolysis-gas chromatography/mass spectrometer (Py-GC/MS) are widely used in determination of functional groups and pyrolysis products in SOC (Polak et al. 2007; De la Rosa et al. 2012). But, till now, there are very few studies that analyzed the light and heavy fractions of SOC using these technologies, especially in biochar application condition.

To consider the information described above, we established a biochar field experiment on calcareous fluvo-aquic soil, beginning from 2009. We determined the water-stable aggregate numbers and TOC and TN contents in different sizes of aggregates, as well as the infrared spectrum and pyrolysis products from light- and heavy-fraction organic matter, to answer the following research questions:

(1) Under field conditions, do different dosages of biochar improve the soil aggregation after 3 years of application?

(2) How does the application of biochar affect the concentration and distribution of organic carbon and nitrogen in different sizes of aggregates?

(3) Can the application of biochar alter the composition of organic carbon in soil aggregates?

2 Materials and methods

2.1 Study site

The long-term field experiment was conducted in the Shangzhuang experimental station of China Agricultural University at Haidian District, Beijing (N 40° 08' 21", E 116° 10' 52"). The experimental field was located on an alluvial plain at an altitude of 51 m and a shallow groundwater level of 1–1.5 m. The region has a typical continental monsoon climate with an annual average air temperature of 11.6 °C and an annual average precipitation of 400 mm. The rainy season generally coincides with the maximum temperatures. Maximum temperatures generally occur in July and minimum temperatures in January. The typical crop planting systems at the study site are winter wheat (from October each year to June the following year) and summer maize (from June to September each year). The test soil is calcareous fluvisol, and the basic soil properties are shown in Table 1. Soil particle distribution was measured by the method of Stemmer et al. (1998), and TOC and TN were analyzed by elemental analyzer (vario EL III, CHNOS Elemental Analyzer, Elementar, Germany). The pH was determined with a glass electrode using a solid-to-water ratio of 1:5 (Lu 2000; Luo et al.

Table 1 The basic properties of soil (0–20 cm) and biochar used in the field experiment

Items	Soil	Biochar
Sand (>0.05 mm), g kg ⁻¹	280	–
Silt (0.05–0.02 mm), g kg ⁻¹	520	–
Clay (<0.02 mm), g kg ⁻¹	200	–
<5-mm particle, g kg ⁻¹	–	950
Organic carbon, g kg ⁻¹	4.32	623 ± 3
Total nitrogen, g kg ⁻¹	0.83	10.5 ± 0.8
C/N	11.7	59.3
CaCO ₃ , g kg ⁻¹	17.3	–
H, g kg ⁻¹	–	43 ± 0.3
Ash, g kg ⁻¹	–	360 ± 3
pH	8.02	10.64 ± 0.01
EC, mS cm ⁻¹	0.185	1.02 ± 0.05
CEC, cmol(+) kg ⁻¹	10.0	12.5 ± 0.1

2011). Soil carbonate was measured by potentiometric titration (Lu 2000). Cation exchange capacity (CEC) by sodium acetate extract (Rhoades 1986), soil solution electrical conductivity (EC), pH, and chloride concentration were determined in a 1:5 soil/water extract.

2.2 Biochar production and experimental design

The biochar used in the experiment was produced with substrate waste from mushroom production. For biochar production, the substrate, a mixture of rice husks (70 %) and cotton seed hulls (30 %), was pyrolyzed at 400 °C for 4 h in a sealed oven. As a commercial biochar-producing system, it had been running for more than 5 years, and its pyrolysis conditions between each oven were almost the same. In the experiment, the biochar was a uniform mixture of a single production of the batch, and the properties of the tested biochar were stable, as shown in Table 1. The analytical method was the same as that of the soil analysis.

The experiment started in June 2009, before the sowing of summer maize. There were four treatments in total: no biochar application (B0) and 30, 60, and 90 t ha⁻¹ biochar applications, shown as B30, B60, and B90. The biochar dosages were equal to 1.11, 2.22, and 3.33 % of the dry mass of the 0–20-cm soil, respectively. There were three repeated plots in each treatment, giving 12 plots in total. The area of each plot was 110 m² and three plots were arranged randomly. Air-dry biochar (~3 % of water content) was uniformly applied on the soil surface to each corresponding plot (oven-dry weight had been corrected) and mechanically plowed into the 0–20-cm soil layer.

The field management patterns of winter wheat and summer maize were the same as that of the local planting model: winter wheat had winter irrigation at early December every year and jointing irrigation in mid-May of the following year. The irrigation method in each case was earth surface broad irrigation with an amount of 900 m³ ha⁻¹. Summer maize was not irrigated during the growing season. Fertilization of both maize and wheat occurred at sowing time at the same fertilization rates of 112.5 N, 112.5 P₂O₅, and 112.5 K₂O kg ha⁻¹. The fertilizer was a compound fertilizer including 15 % content each for N, P₂O₅, and K₂O. Each June, wheat straws were mechanically crushed into 2–3-cm pieces and mulched over the soil surface during the grain harvest. Each October, maize straws were also mechanically smashed into 1–2-cm pieces and plowed into the 0–20-cm soil layer during the grain harvest.

On October 10, 2012, before the summer maize harvesting, soil samples from the 0–20-cm soil layer were randomly collected by soil auger (3 cm diameter). In each plot, 10–13 auger samples were taken and mixed well, and a 2-kg compost sample was extracted for analysis. After the natural air-drying,

large materials such as stones and residual roots were picked out, and the soil samples were screened through a 5-mm sieve.

2.3 Separation of soil water-stable aggregates

The wet-sieving procedure of Elliott (1986) was used to separate soil water-stable aggregates. Soil samples from B0, B30, B60, B90, and initial (sampled in 2009 before the experiment) were separated into water-stable aggregates of different sizes. Considering the stability of soil aggregates was usually consistent in the determined soil condition, we tried to use one plot sample to separate the aggregates, but the quantity of >1000 µm was insufficient to do the following analysis, like TOC, TN, FTIR, and Py–GC/MS. To get sufficient subsamples of each size of aggregates, two soil samples from two plots of the same treatment were used in the separation; then, the two subsamples were mixed together. Briefly, an 80.00-g sample was placed in the plan sieve, applied to the automatic oscillatory device (TTF-100 model, vertical stroke is 40 mm, and the frequency is 1–40 rounds per minute), and shaken for 8 min at room temperature (30 rounds per minute). Deionized water was used to elute the soil. Aggregates that remained on the sieves of 1000, 250, and 53 µm were >1000, 1000–250, and 250–53 µm, respectively. The soil in the suspension liquid was regarded as aggregates smaller than 53 µm in diameter. All separated subsamples were placed in an aluminum specimen box with known weight and left to stand for 24 h. We then discarded the liquid supernatant and dried the subsamples at 60 °C for 24 h, after which the subsamples were weighed.

Mean weight diameter was calculated using the following formula:

$$MWD = \sum_{i=1}^n \bar{x}_i \cdot W_i \quad (1)$$

in which \bar{x}_i represents the mean diameter of each size of aggregates, and W_i represents the weight percentage of size i of the aggregates.

2.4 Separation of organic carbon components in light and heavy fractions of soil

The improved method of Golchin et al. (1994) was used to determine the organic carbon in the heavy fraction, free state, and occluded light fractions of soil. The detailed operation steps were as follows:

- (1) The 10.00-g aggregates obtained from the procedure described in the previous section were put into 50-ml plastic centrifuge tubes, to which 50 ml NaI solution was added ($d=1.8 \text{ g cm}^{-3}$), gently hand shaken, and left to stand overnight at room temperature. The next day, this mixture was centrifuged for 15 min at 3500 rpm and filtered using a 0.45-µm membrane by air pump. The

0.01 M CaCl₂ solution and distilled water were used to elute the soil fraction which stayed on the filter membrane. The substance eluted was treated with 50 ml NaI solution, and the previous process was repeated. Finally, the substance eluted was dried at 60 °C and weighed to yield the free-state light-fraction components.

- (2) Next, 50 ml NaI solution was added to the precipitate in the centrifuge tube, shaken well, treated with ultrasonic dispersion for 15 min, centrifuged, and pump filtered with sintered glass filter twice as above. The soil that remained on the filter membrane was eluted and collected, dried, and weighed to obtain the occluded light-fraction components. These were merged with the free-state light-fraction components from step 1 to form the light fraction (LF) of soil aggregates.
- (3) Then, 50 ml of distilled water was added to the precipitates in centrifuge tubes, shaken well for 20 min, and then centrifuged for 20 min. The precipitates in centrifuge tubes were washed repeatedly until colorless with 95 % ethyl alcohol, then dried and weighed to give the heavy-fraction (HF) components.

2.5 TOC and TN contents

TOC and TN of bulk soil and aggregate samples of B0, B30, B60, B90, and initial were measured by CHNOS elemental analyzer (vario EL III, CHNOS Elemental Analyzer, Elementar, Germany) after removing carbonate. Briefly, 50 ml 1 M HCl and 5 g soil (10:1) were mixed for 24 h and then centrifuged at 3000 rpm for 5 min. The supernatant was discarded and 50 ml distilled water was added to wash the soil, then centrifuged at 3000 rpm for 5 min, and this step was repeated twice. The sample was placed in an oven at 60 °C

for 24 h. Forty- to sixty-milligram dried samples were used to analyze TOC and TN contents.

2.6 FTIR

Fourier transform infrared (FTIR) spectra of LF and HF of the aggregates of initial and B0 and B90 biochar used in this study were recorded from pellets containing 1.5 mg of the oven-dried soil LF or HF samples with 150 mg of dry KBr. The instrument used was a Nicolet 5PC FTIR spectrophotometer covering a wavenumber range of 400–4000 cm⁻¹ in 2 cm⁻¹ intervals. The main absorbance bands in the FTIR spectra and their assignments are shown in Table 2. The spectra of biochar are shown in Fig. 1.

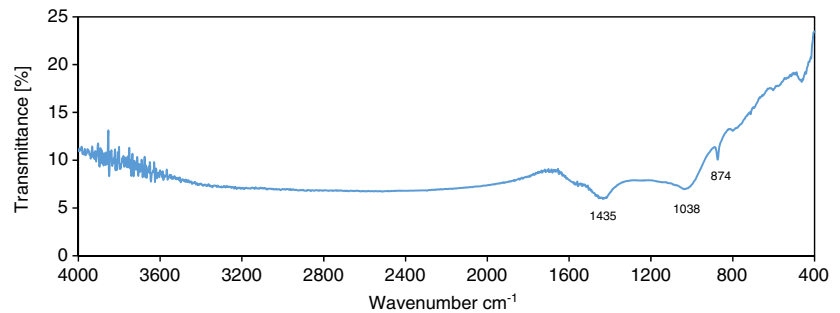
2.7 Py–GC/MS

Analytical pyrolysis (Py–GC/MS) samples were the same as those of FTIR, and they were performed using an electrically heated platinum filament CDS 1000 pyroprobe valve interfaced to a Varian 3400 GC equipped with a GC column (HP-5-MS; Agilent Technologies 30 m × 0.25 mm, 0.5 μm) and a mass spectrometer (Saturn 2000 ion trap, Varian Instruments). The GC thermal program was 50 to 300 °C at 5 °C min⁻¹; the MS conditions were electron ionization at 70 eV and full scan acquisition in the 15–550 *m/z* interval. A quartz sample tube containing 1 mg sample was inserted into the Py–GC interface (280 °C) and then pyrolyzed at 650 °C (set temperature) for 10 s with helium as carrier gas (1 ml min⁻¹). The MS spectrum was compared to standards in NIST 11 Database composed of ca. 240,000 standard spectra. Of the pyrolysis products, they were quantified using the peak area of their characteristic fragment ions. This semi-quantitative dataset provides relative contributions of the

Table 2 Assignment of the principal descriptive IR absorption bands

Wavenumber (cm ⁻¹)	Proposed assignment	Reference
3432–3416	Stretching vibration of the O–H bond of carboxyl and hydroxyl groups, or water, alcohols, and phenols	Ellerbrock and Gerke (2004), Simkovic et al. (2008)
2925–2922	Aliphatic stretching vibration of C–H	Ellerbrock and Gerke (2004), Simkovic et al. (2008)
1636–1570	Aromatic C=C	Calderón et al. (2013), Pedersen et al. (2011)
1435	Stretching vibration of CO ₃ ²⁻ in carbonates	Rossel and Behrens (2010), Soriano-Disla et al. (2014)
1384	Stretching vibration of C–H in methyls	Rossel and Behrens (2010)
1038–1032	Stretching of Si–O	Soriano-Disla et al. (2014)
900–675	Out-of-plane bending of the aromatic ring C–H bonds in aromatics	Smidt and Meissl (2007)

Fig. 1 FTIR spectra of biochar used in the study. Note: 1435, 1038, and 874 cm^{-1} peaks attributed to carbonate, stretching of Si–O, and out-of-plane bending of the aromatic ring C–H bonds, respectively



pyrolysis products expressed as a proportion (%) of the total quantified peak area (TQPA), which allows a more detailed comparison between samples than from visual inspection of pyrograms alone. The total ion chromatograms from Py–GC/MS of biochar used in the study are shown in Fig. 2.

2.8 Statistic

The soil aggregate concentration of TOC or TN was measured by elemental analyzer directly, which means the concentration of TOC or TN in each size of soil aggregates. The soil aggregate amount of TOC or TN means the TOC amount in the bulk soil, which is equal to the TOC or TN concentration in the determined aggregate size by distribution ratio of the aggregate in the bulk soil.

Soil aggregate distribution data analysis was performed using R (R i386 3.0.2) software to conduct one-way analysis of variance ($p < 0.05$), and the Duncan method was applied to do multiple comparisons between the different treatments. Principal component analysis (PCA) is a method used to consider a multivariate data set based on the variance of the data set rather than the variance of any one measured variable. Principal component analysis (White et al. 2007; Carr et al. 2013) was applied to analyze the differences of Py–GC/MS

pyrolysis products between all sizes of aggregates under various treatments.

3 Results

3.1 Distribution and stability of soil aggregates

Before the initiation of the experiment (initial), the percentages (aggregate mass in the bulk soil) of aggregates with sizes of >1000 and 1000 – 250 μm were 7.1 and 28.9 %, respectively (36 % in total). After commencement of the experiment, the percentages of aggregates with sizes of >1000 and 1000 – 250 μm were significantly decreased by the B0 treatment; the two totaled only 14.4 %, giving a decrease of 60 % from initial values. After the application of biochar, compared to B0, the percentage of the >1000 - μm aggregates increased by 75 % (B30), 210 % (B60), and 225 % (B90), in which the treatments of B60 and B90 showed non-significant differences from the level before the experiment ($p < 0.05$). The B60 treatment substantially increased the percentage of the 1000 – 250 - μm aggregates. The percentage of the >250 - μm aggregates under the treatments of B60 and B90 reached 28.6 and 16.7 %, respectively, and increased by 99 and 16 %, respectively, compared with the B0 treatment. The

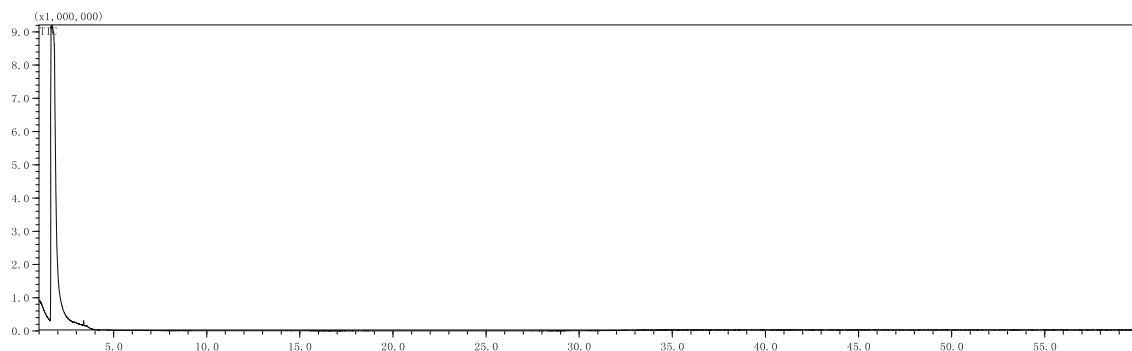


Fig. 2 Total ion chromatograms from Py–GC/MS of biochar used in the study. Note: The main peak stands for CO_2 which accounts for more than 99 % in the total pyrolysis products

mean weight diameter under the treatments of B60 and B90 increased by 52 and 12 %, respectively, compared with that under the B0 treatment. These results showed that the application of 60–90 t ha⁻¹ biochar can effectively reduce the breakage of soil macro-aggregates, especially at the optimal dosage of 60 t ha⁻¹ (Table 3).

3.2 Concentration distribution of TOC and TN in aggregates

Biochar can considerably increase the TOC concentration of soil macro-aggregates (>250 μm). In the >1000-μm aggregates, the TOC concentrations were 48.98 g kg⁻¹ (B30), 54.13 g kg⁻¹ (B60), and 106.77 g kg⁻¹ (B90) after the application of biochar, and the increases were 44, 59, and 215 %, for B30, B60, and B90, respectively, compared with 33.94 g kg⁻¹ in the B0 treatment. Similarly, in the 1000–250-μm aggregates, the biochar increased the TOC concentration by 61 % (B30), 42 % (B60), and 242 % (B90). In the aggregates with sizes of 250–53 and <53 μm, the application of biochar also increased the TOC concentration (Fig. 3).

The effect of biochar on the TN concentration was consistent with that on the TOC in aggregates, which significantly increased the concentration of TN in macro-aggregates but had a minor effect on micro-aggregates. In the >1000-μm aggregates, the TN concentration was 2.28, 2.30, and 3.97 g kg⁻¹ in the B30, B60, and B90 treatments, respectively, and increased by 35, 36, and 135 %, respectively, compared with 1.69 g kg⁻¹ in the B0 treatment. In the 1000–250-μm aggregates, the treatments of B30, B60, and B90 increased the TN concentrations by 24, 4, and 108 %, respectively, and the maximum value was 2.62 g kg⁻¹ in the B90 treatment.

The application dosage of biochar showed a significant positive correlation with the concentrations of soil TOC and TN ($p < 0.05$). The TOC concentrations in B30, B60, and B90 increased by 57, 97, and 155 %, respectively, compared with 6.12 g kg⁻¹ in the B0 treatment. Different dosages of biochar

increased the TN concentration by 13 % (B30), 27 % (B60), and 39 % (B90).

The amount distribution of TOC and TN in soil aggregates was determined by aggregate mass ratio and TOC or TN concentration. Biochar increased the content and ratio of TOC or TN in macro-aggregates, which can be notably increased with increasing biochar application rate. In the >1000-μm aggregates, the TOC concentrations were increased by 152, 400, and 942 % under the B30, B60, and B90 treatments, respectively, compared with 0.67 g kg⁻¹ in the B0 treatment. Moreover, the TN concentrations were increased by 138, 329, and 683 % with biochar application for the B30, B60, and B90 treatments, respectively, compared to 0.03 g kg⁻¹ in the B0 treatment. In the 1000–250-μm aggregates, the TOC concentrations were increased by 44, 158, and 182 %, and the TN concentrations were increased by 11, 88, and 71 % for the B30, B60, and B90 treatments, respectively (Table 4).

In addition, biochar could increase the proportion of macro-aggregate TOC or TN in whole soil TOC or TN. The application of 90 t ha⁻¹ biochar had the most effect on the ratios of TOC and TN in the >1000-μm aggregates, which were raised from 11 and 4 % to 44 and 24 %, respectively. In the 1000–250-μm aggregates, the application of 60 t ha⁻¹ biochar had a clear effect on both, which were raised from 27 and 19 % to 36 and 31 % for TOC and TN, respectively.

With the biochar application amount increasing, the soil C/N showed a significant increasing trend ($p = 0.01$). B30, B60, and B90 increased C/N by 38, 55, and 84 %, respectively, compared with B0 at 8.16. Each treatment increased C/N in all sizes of aggregates. C/N in the >53-μm aggregates was related to the biochar application amount and significantly increased with the increasing biochar application amount. The soil C/N showed a significant increasing trend in the >1000-μm ($p = 0.019$), 1000–250-μm ($p = 0.024$), and 250–53-μm ($p = 0.03$) aggregates.

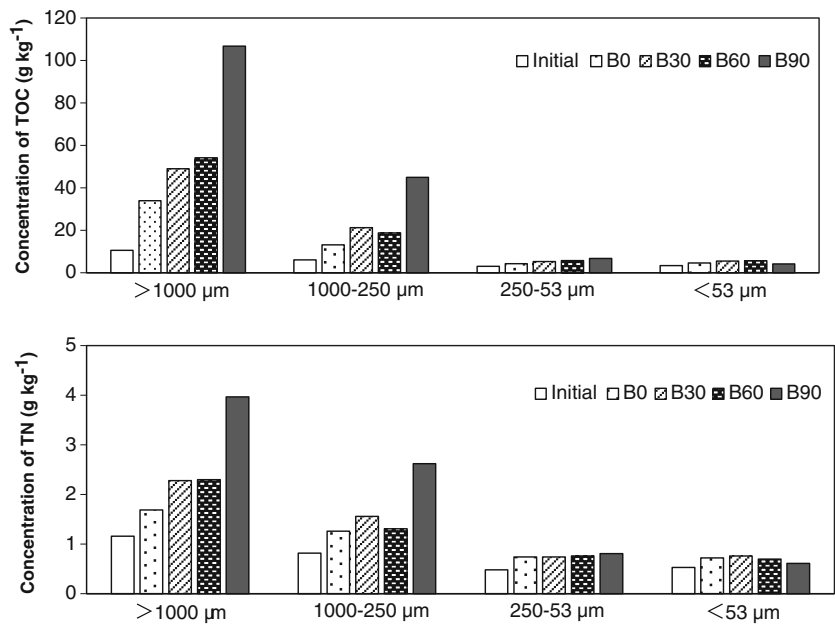
Table 5 shows that each treatment increased the TOC content in light and heavy fractions of aggregates except for the TOC in the heavy fraction of the 250–53-μm aggregates. The

Table 3 The effect of biochar amendment on the size distribution and mean weight diameter (MWD) of soil aggregates

Treatments	Aggregate size (μm), %				MWD μm
	>1000	1000–250	250–53	<53	
Initial	7.1 ± 0.1 a	28.9 ± 2.5 a	38.1 ± 6.5 a	25.9 ± 4.2 a	316.1 ± 5.2 a
B0	2.0 ± 0.2 b	12.4 ± 2.6 ab	40.2 ± 6.2 a	45.5 ± 9.0 a	170.0 ± 25.3 b
B30	3.5 ± 0.8 b	11.1 ± 3.0 b	50.2 ± 2.4 a	35.2 ± 4.7 a	189.2 ± 13.5 b
B60	6.2 ± 0.1 a	22.4 ± 0.4 ab	30.2 ± 0.8 a	41.2 ± 2.6 a	258.7 ± 19.3 ab
B90	6.5 ± 0.1 a	10.2 ± 0.5 b	31.3 ± 0.9 a	52.0 ± 1.5 a	190.4 ± 5.0 b

Note: The mean values in each column followed by the different letters are different significantly at $p < 0.05$ level. B0, B30, B60, B90, and Initial stand for soil amendment with 0, 30, 60, and 90 t ha⁻¹ biochar and the soil before biochar amendment in 2009, respectively

Fig. 3 The concentration of TOC and TN in soil aggregates. Note: The aggregate concentrations of TOC and TN were measured by elemental analyzer directly, which means the TOC and TN concentrations in each size aggregate. *B0*, *B30*, *B60*, *B90*, and *Initial* stand for soil amendment with 0, 30, 60, and 90 t ha⁻¹ biochar and the soil before biochar amendment in 2009. *TOC* total organic carbon, *TN* total nitrogen



TOC content in light and heavy fractions of the >1000-μm aggregates as well as the light fraction of the 1000–250-μm aggregates showed a significant positive correlation with the biochar application amount. In light-fraction components of the >1000-μm aggregates, the TOC contents were 8 times, 28 times, and 27 times those under B0 treatment for B30, B60, and B90, respectively. In heavy-fraction components, they were 5 times, 13 times, and 17 times those of B0 for B30, B60, and B90, respectively.

Similar to TOC, the TN content in light and heavy fractions of the >1000-μm aggregates as well as the light fraction of the 1000–250-μm aggregates showed significant positive correlation with the biochar application amount. In the light-fraction components of the >1000-μm aggregates, the TN contents were 7 times, 22 times, and 29 times those under B0 treatment for B30, B60, and B90, respectively. In the heavy-fraction components, they were 4 times, 8.7 times, and 10.5 times those of B0 for B30, B60, and B90, respectively.

The aggregate C/N was between 7.43 and 37.39, and C/N in light fractions of aggregates with different diameters was larger than the corresponding heavy fraction. With the increasing biochar application amount, C/N in light fractions of aggregates with different diameters and heavy fractions of the >1000-μm aggregates were increased. Compared with B0, the B90 treatment increased the C/N in light fractions of aggregates with different diameters by 30, 56, 55, and 49 %. Different biochar dosages increased the C/N in heavy fractions of the >1000-μm aggregates by 28, 46, and 57 %, respectively.

3.3 FTIR

Infrared spectroscopy is an effective tool to study the structure and properties of compounds, with wide application in soil organic carbon analysis. Figure 4 gives the spectrograms of light and heavy fractions of soil aggregates under the initial and B0 and B90 treatments.

The spectra of the 24 soil aggregate samples featured the most common peaks except for some specific ones that are marked in Fig. 4. The interpretation of the major peaks was based on Table 2. The spectra peak featured at 3432–3416 cm⁻¹ was attributed to stretching vibration of the O–H bond in carboxyl and hydroxyl groups, and around 2925 and 1384 cm⁻¹ peaks stood for the stretching vibration of aliphatic C–H, typically methyl and methylene. The aromatic C=C bands appeared at a peak of 1636–1570 cm⁻¹, while the largest peak of near 1032 cm⁻¹ was defined as stretching vibration of Si–O. There is out-of-plane bending of the aromatic ring C–H bonds found at 900–675 cm⁻¹.

In Fig. 4, the difference among the three treatments decreased as the soil aggregate size decreased, regardless of whether in the light fraction or heavy fraction. In the same size of soil aggregates, the light fraction differed from the heavy fraction. The peak at 1384 cm⁻¹ only existed in the light fraction except for the heavy fraction of the >1000-μm aggregates in B90, while the heavy fraction included 795 cm⁻¹ peaks which were not found in the heavy fraction of the >1000-μm aggregates. In addition, the peak of 2922 cm⁻¹ in the light fraction was higher than that of the heavy fraction. Biochar only had influence on the 1384 cm⁻¹ peak in

Table 4 The amount of organic C and total N in soil aggregates and its proportion to the bulk soil

	Treatments	Bulk soil (g kg ⁻¹)	Soil aggregates (μm) (g kg ⁻¹ soil)				Recovery ratio (%)
			>1000	1000–250	250–53	<53	
TOC	Initial	4.32	0.75 (17)	1.77 (39)	1.15 (25)	0.87 (19)	105
	B0	6.12	0.67 (11)	1.63 (27)	1.72 (28)	2.11 (34)	100
	B30	9.58	1.69 (20)	2.35 (27)	2.66 (31)	1.96 (23)	90
	B60	12.03	3.35 (29)	4.20 (36)	1.72 (15)	2.33 (20)	96
	B90	15.60	6.98 (44)	4.60 (29)	2.10 (13)	2.15 (14)	101
TN	Initial	0.62	0.08 (13)	0.24 (37)	0.18 (29)	0.14 (22)	103
	B0	0.75	0.03 (4)	0.16 (19)	0.30 (37)	0.33 (40)	109
	B30	0.85	0.08 (9)	0.17 (19)	0.37 (42)	0.27 (30)	105
	B60	0.95	0.14 (15)	0.29 (31)	0.23 (24)	0.29 (30)	100
	B90	1.04	0.26 (24)	0.27 (24)	0.25 (23)	0.32 (29)	106
C/N	Initial	6.97	9.13	7.45	6.27	6.32	
	B0	8.16	20.08	10.44	5.78	6.46	
	B30	11.27	21.48	13.60	7.15	7.32	
	B60	12.66	23.53	14.29	7.49	8.07	
	B90	15.00	26.89	17.17	8.28	6.77	

Note: Soil aggregates' amount of TOC or TN means the TOC amount in the bulk soil, which is equal to the TOC or TN concentration in determined size aggregate by distribution ratio of the aggregate in the bulk soil. The data in parentheses indicates the proportion of organic carbon or total nitrogen in the corresponding aggregate to that of the bulk soil. B0, B30, B60, B90, and Initial stand for soil amendment with 0, 30, 60, and 90 t ha⁻¹ biochar and the soil before biochar amendment in 2009, respectively

TOC total organic carbon, TN total nitrogen, C/N ratio of total organic carbon to total nitrogen

the heavy fraction of the >1000-μm aggregates, but it eliminated or decreased the peak height at 3420 and 2922 cm⁻¹, which indicated that biochar could increase the methyl content in the heavy fraction of large aggregates and decrease the O–H content in carboxyl and hydroxyl groups.

3.4 Py–GC/MS

There were 90 pyrolysis products of aggregate light fraction components (Appendix 1, Electronic Supplementary Material) and 72 heavy fractions (Appendix 2, Electronic Supplementary Material). Several categories were classified according to the sources of small molecular compounds: (1) *n*-alkanes/enes pairs (Alk); (2) aromatic structures, mainly composed of benzenes and naphthalenes (Ar); (3) polysaccharides-derived compounds, mostly comprising furanes (Ps); (4) N-containing products derived from peptides; (5) fatty acid methyl esters (FAMEs); (6) *n*-alkyl ketones (K); (7) *n*-alkane nitriles (AN); (8) lignin-derived products (Lg); and (9) triterpenoids and sterols that are possibly derived from plant material (De la Rosa et al. 2012). The total percentage of CO₂, Alk, Ar, Ps, and Lg reached 76.6–99.5 %. Since other substances merely constitute 7 % in average, only the above five groups of compounds were analyzed.

Principal component analysis on the five substances in the light fraction components was conducted, and results showed that the first two principal components could reach a resolution of 81 %. In the first principal component, both the load values of Lg and Ps were –0.60, indicating that with greater *x*-axis values the contents of Lg and Ps decrease. The load values of Alk, Ar, and CO₂ in the second principal component were 0.605, 0.497, and –0.611, respectively, indicating with greater *y*-axis values the contents of Ar and Alk increase while CO₂ content decreases (Fig. 5). Figure 5 shows the B0 distribution was rather dispersed, and the pyrolysis products of the >1000-μm aggregates were more enriched in CO₂, while those of the 1000–250- and <53-μm aggregates were more enriched in Lg and Ps, and those of the 250–53-μm aggregates were more enriched in Alk. After the application of biochar (B90), all the pyrolysis products were located on the positive side of PC1, indicating biochar increased both CO₂ and Alk contents.

The principal component analysis results of heavy-fraction pyrolysis products showed the resolution of the first principal component was 47 % with Ar and Lg as positive load as well as CO₂ and Ps as negative load. The resolution of the second principal component was 30 % with a maximum load value of Alk (0.731), and the load values of Lg and Ps were negative.

Table 5 The amount of organic C and total N in the light and heavy fractions in soil aggregates and its proportion to the bulk soil

Fraction	Aggregates (µm)	Initial	B0	B30	B60	B90
TOC (g kg ⁻¹)	LF	0.43 (8.7)*	0.21 (4.3)	1.76 (17.3)	5.88 (36.3)	7.80 (40.0)
	1000–250	0.48 (9.7)	0.27 (5.6)	1.24 (12.2)	2.06 (12.7)	2.49 (12.8)
	250–53	0.08 (1.6)	0.16 (3.3)	1.05 (10.3)	0.67 (4.1)	0.18 (0.9)
	<53	0.19 (3.8)	0.13 (2.7)	0.66 (6.5)	1.00 (6.2)	1.21 (6.2)
	In total	1.18 (23.8)	0.77 (15.9)	4.71 (46.3)	9.61 (59.3)	11.68 (59.9)
	HF	0.42 (8.5)	0.16 (3.3)	0.79 (7.8)	2.04 (12.6)	2.64 (13.5)
	1000–250	1.31 (26.5)	1.04 (21.5)	1.08 (10.6)	1.80 (11.1)	1.27 (6.5)
	250–53	0.90 (18.2)	1.29 (26.7)	1.76 (17.3)	1.10 (6.8)	1.10 (5.6)
	<53	1.13 (22.9)	1.58 (32.6)	1.83 (18.0)	1.63 (10.1)	2.81 (14.4)
	In total	3.76 (76.1)	4.09 (84.1)	5.40 (53.7)	6.57 (40.6)	7.82 (40)
TN (mg kg ⁻¹)	LF	25.0 (4.8)	7.3 (1.6)	53.7 (7.3)	163.2 (18.8)	208.6 (23.5)
	1000–250	26.6 (5.1)	15.1 (3.3)	52.1 (7.1)	75.3 (8.7)	89.0 (10.0)
	250–53	4.5 (0.9)	8.7 (1.9)	44.5 (6.1)	24.0 (2.8)	6.3 (0.7)
	<53	7.6 (1.5)	6.6 (1.4)	28.1 (3.8)	34.4 (4.0)	41.2 (4.6)
	In total	63.7 (12.3)	37.7 (7.2)	178.4 (24.3)	296.9 (34.3)	345.1 (38.8)
	HF	45.3 (8.7)	9.1 (2.0)	35.0 (4.8)	79.3 (9.1)	95.5 (10.8)
	1000–250	142.9 (27.5)	84.5 (18.4)	84.2 (11.5)	168.4 (19.4)	83.4 (9.4)
	250–53	121.2 (23.3)	132.2 (28.8)	233.6 (32.0)	146.8 (16.9)	84.2 (9.5)
	<53	147.3 (28.3)	194.8 (42.5)	199.5 (27.3)	175.8 (20.3)	278.6 (31.4)
	In total	456.7 (87.8)	420.6 (91.7)	552.3 (75.6)	570.3 (65.7)	541.7 (61.1)
C/N	LF	17.20	28.77	32.77	36.03	37.39
	1000–250	18.05	17.88	23.80	27.36	27.98
	250–53	17.78	18.39	23.60	27.92	28.57
	<53	25.00	19.70	23.49	29.07	29.37
	>1000	9.27	17.58	22.57	25.73	27.64
	1000–250	9.17	12.31	12.83	10.69	15.23
	250–53	7.43	9.76	7.53	7.49	13.06
	<53	7.67	8.11	9.17	9.27	10.09

Note: Soil aggregates' amount of TOC or TN means the TOC amount in the bulk soil, which is equal to the TOC or TN concentration in determined size aggregate by distribution ratio of the aggregate in the bulk soil. The data in the parentheses indicates the proportion of organic carbon or total nitrogen in the corresponding aggregates to that of the bulk soil. B0, B30, B60, B90, and Initial stand for soil amendment with 0, 30, 60, and 90 t ha⁻¹ biochar and the soil before biochar amendment in 2009, respectively

LF light fraction in the aggregates, HF heavy fraction in the aggregates, TOC total organic carbon, TN total nitrogen, C/N ratio of total organic carbon to total nitrogen

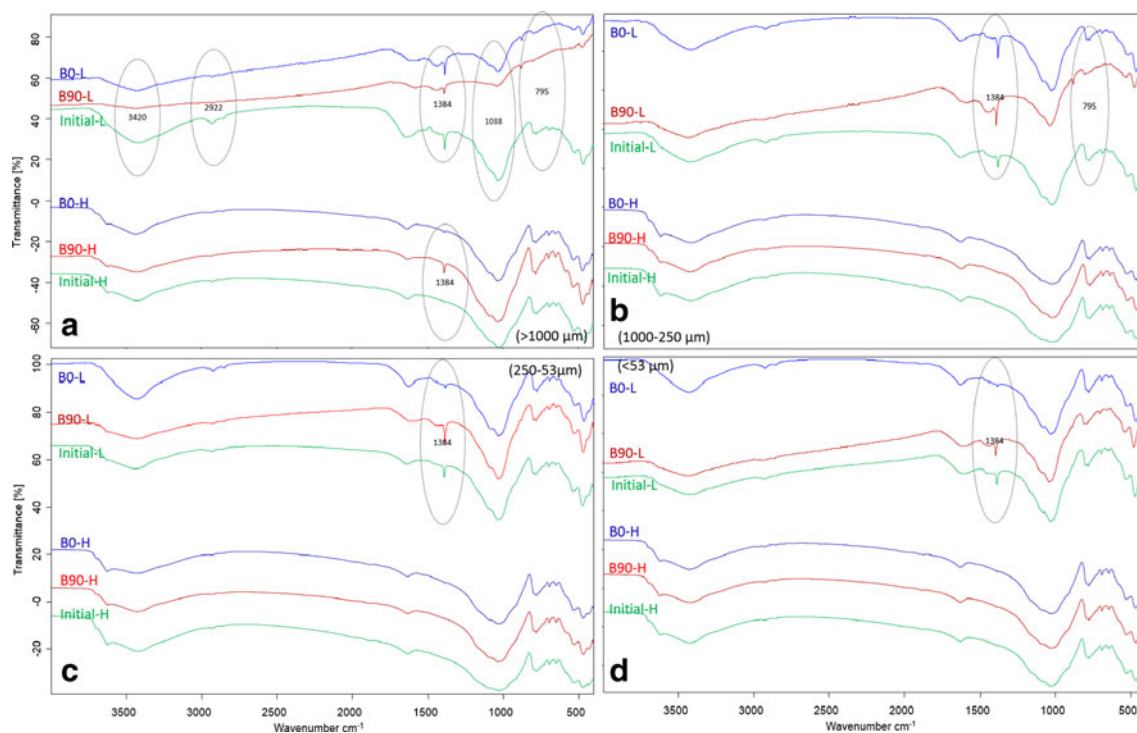


Fig. 4 The FTIR spectra of the light and heavy fractions in soil aggregates. Note: **a**, **b**, **c**, and **d** are the different aggregate hierarchies, indicating >1000-, 1000–250-, 250–53-, and <53- μm aggregates, respectively. *B0*, *B90*, and *Initial* stand for soil amendment with 0 and

90 t ha^{-1} biochar and the soil before biochar amendment in 2009, respectively. *L* means light fraction whereas *H* means heavy fraction in the aggregates

Figure 3b shows that each size of the aggregates under the B0 treatment was generally distributed in the lower quadrant, indicating a lower content of Alk. However, it was higher in the >1000- and 250–53- μm aggregates of B90 with biochar application.

4 Discussion

4.1 Effects of biochar on soil water-stable aggregates

(1) Biochar can reduce the breakage of soil macro-aggregates. Soil tillage and application of fertilizers have been shown to break the soil aggregates (Angers et al. 1993; Fonte et al. 2009), a result that was confirmed in this study. Compared with the initial soil (years of rice cultivation), the yearly tillage and fertilizer applications (B0) resulted in a decrease in the proportion of the >1000- μm soil aggregates from 7.1 to 2.0 %, and reduction of soil MWD by 46 % (Table 3). However, with the increase in biochar application, the proportion of the >1000- μm soil aggregates increased gradually after 3 years, and reached 6.5 % at the dosage of 90 t ha^{-1} , close to the level of the initial soil

(Table 3). At the same time, the soil MWD also showed an increasing trend, indicating that biochar addition can reduce the breakage of soil macro-aggregates.

(2) The mechanisms of the impact of different biochar dosages on soil aggregate distribution. The most widely accepted theory of soil aggregation of primary soil particles is the stage theory by Tisdall and Oades (1982). This states that soil micro-aggregates are generated from soil mineral particles through binding of multivalent ions and soil organic matter. The soil micro-aggregates are held together by plant roots and fungal hyphae, gradually forming different sizes of aggregates (Tisdall and Oades 1982). At present, the main theory of soil aggregate turnover is the conceptual model proposed by Six et al. (2000), which states that (1) macro-aggregates are scattered by tillage mechanical forces to form micro-aggregates; (2) POMs in macro-aggregates are degraded by microorganisms to form new micro-aggregates, releasing the originally bounded micro-aggregates into free micro-aggregates; and (3) when organic residues are added, the above micro-aggregates are transformed back into macro-aggregates.

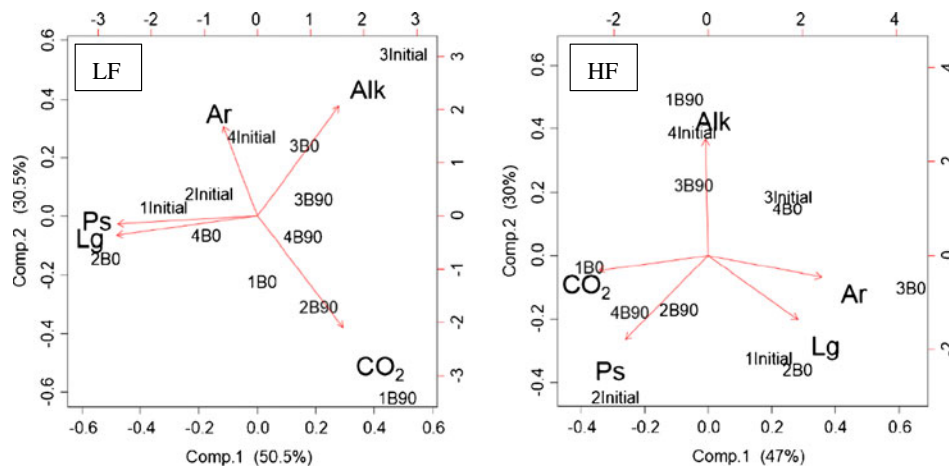


Fig. 5 The PCA of Py–GC/MS sources of the light fraction (LF) and heavy fraction (HF) in soil aggregates in the soils of the *Initial* and *B0* and *B90* treatments. Note: 1, 2, 3, and 4 are the different aggregate hierarchies, indicating >1000-, 1000–250-, 250–53-, and <53- μ m aggregates, respectively. *B0*, *B90*, and *Initial* stand for soil amendment with 0 and

90 t ha⁻¹ biochar and the soil before biochar amendment in 2009, respectively. *LF* means light fraction whereas *HF* means heavy fraction in the aggregates. *Alk*, *Ar*, *Ps*, and *Lg* codes refer to molecules derived from *n*-alkanes/enes, aromatic compounds, polysaccharides, and lignin, respectively

We raise the following hypotheses regarding the influence mechanisms of different amounts of biochar on soil aggregate turnover (Fig. 6):

- With an increasing amount of biochar application, biochar particles successively react with the <53- μ m particles, micro-aggregates (53–250 μ m), and then macro-aggregates (250–1000 μ m), but not with exceptionally large macro-aggregates (>1000 μ m).
- Biochar particles could cause the <53- μ m particles and micro-aggregates to gradually aggregate. That is, the <53- μ m particles would aggregate into micro-aggregates, and micro-aggregates would aggregate into macro-aggregates.
- Biochar particles could cause disintegration of macro-aggregates into the <53- μ m particles, which is described as follows. This study focuses on different sizes of aggregates that already exist in the soil before the application of biochar. Among these, the <53- μ m particles accounted for 26 %, micro-aggregates for 38 %, macro-aggregates for 29 %, and larger macro-aggregates for 7 % (Table 3). When small amounts of biochar particles were added to the soil (e.g., 30 t ha⁻¹), they were mainly in contact with the <53- μ m particles (Fig. 6a). The contact between the biochar and the <53- μ m particles cemented into micro-aggregates, which caused an increase in the number of micro-aggregates and a subsequent decrease in the <53- μ m particles (Table 3). When medium amounts of biochar particles were added to the soil (e.g., 60 t ha⁻¹), they interacted with the <53- μ m particles and micro-aggregates simultaneously (Fig. 6b). This caused

cementation to form micro-aggregates for interactions with the <53- μ m particles and macro-aggregates for interactions with micro-aggregates. Therefore, the number of macro-aggregates increased, while the number of micro-aggregates was determined by the net effect of the formation and upward aggregation (and thus reduction). Therefore, because the amount of the <53- μ m particles forming micro-aggregates was relatively low, the 60 t ha⁻¹ treatment reduced the number of soil micro-aggregates and raised the number of macro-aggregates (Table 3). When a large amount of biochar particles was added to the soil (e.g., 90 t ha⁻¹), they were in contact with three different sizes of particles (Fig. 6c). The net changes in the number of these particles were calculated by the net effect of formation and loss. In this study, macro-aggregates decreased about 10 % (compared with B60), the <53- μ m particles increased about 10 %, and micro-aggregates remained relatively unchanged (Table 3).

The evidence supporting hypothesis (3) includes the following: (1) the stage theory by Tisdall and Oades (1982) and the aggregate turnover model by Six et al. (2000); (2) the majority of the biochar particles were less than 5 mm and were therefore mainly in contact with the soil micro-particles, and steady contact with the >1000- μ m particles was difficult to maintain (Brodowski et al. 2006); (3) the surface of the soil clay particles and the surface of the biochar particles can be connected through the surface hydroxyl and phenolic hydroxyl groups of the biochar particles (Lin et al. 2012; Soinne et al. 2014); (4) the stable chemical properties of sand (quartz) (Zelazny et al. 1996) make it difficult to bind with clay minerals or SOM (biochar) (Bühmann et al. 2006); (5) extra

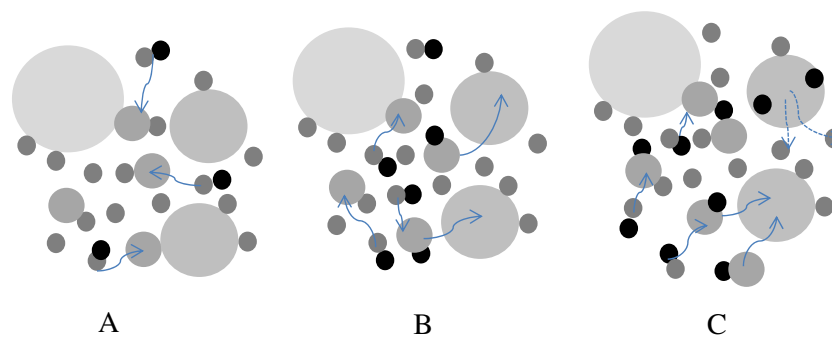


Fig. 6 The mechanism of biochar in different amounts affects the soil aggregate formation process. Note: The *black points* stand for the biochar particle, and each *black point* is equal to 10 t biochar in a 1-ha field. The *gray points* refer to soil aggregates and different point sizes stand for different soil aggregates. **a** illuminates a small amount of biochar contacting only with $<53\text{-}\mu\text{m}$ particles, making them into micro-

aggregates; **b** illuminates a middle amount of biochar contacting with both $<53\text{-}\mu\text{m}$ and micro-aggregates, making them into bigger aggregates. **c** shows a large amount of biochar contacting with $<53\text{-}\mu\text{m}$, micro-, and big aggregates, making $<53\text{-}\mu\text{m}$ and micro-aggregates into bigger ones and breaking big aggregates into $<53\text{-}\mu\text{m}$ particles

macro-aggregates can be disintegrated into the $<53\text{-}\mu\text{m}$ particles. De Gryze et al. (2006) showed that 3 weeks after culture conditions, roughly 30 % of extra macro-aggregates had disintegrated into the $<53\text{-}\mu\text{m}$ particles.

(3) Effect of biochar on soil aggregate turnover under field conditions

Soil properties, such as soil texture, clay mineral species, SOM content, cations, oxides, and carbonates, are the most important factors that affect field soil aggregation and aggregate stability (Le Bissonnais 1996; Six et al. 2004; Bronick and Lal 2005; Plaza-Bonilla et al. 2013). The sandy loam soil used in this study was low in both organic matter content and CEC and included 2:1 type clay minerals (Table 1). These properties are not conducive to the formation of soil macro-aggregates (Oades 1993; Le Bissonnais 1996; Kay 1998; Deneff et al. 2002; Lado et al. 2004; Dimoyiannis 2012). In this case, it is therefore reasonable that the use of biochar does not significantly increase soil aggregation (Table 3), and this does not contradict the result that biochar promotes the aggregation of clay soil or rich almandine soil (Liu et al. 2012; Awad et al. 2013; Soinnie et al. 2014).

Using a single sampling time to evaluate the effect of a long-term field experiment has natural flaws, especially if assessment of seasonal and/or interannual variation is desired. Under field conditions, the dynamics of soil aggregates can be influenced by the freeze–thaw cycle (Lehrsch et al. 1991), alternating wet and dry climates (Dalal and Bridge 1996), rainfall (Guto et al. 2011), crop growth (Jastrow et al. 1998), straw returns (Abiven et al. 2009; Chivenge et al. 2011), and seasonal variations (Guto et al. 2011; Plaza-Bonilla et al. 2013). In addition, the dynamic changes of soil aggregation are also affected

by interannual climate changes. Taken together, these factors make it difficult to elucidate the real effect of treating factors in field studies. In this present study, the following factors have been neglected: (1) the sampling time of this study was before the summer maize harvest, which was 3 months since the last straw return of winter wheat. The effects of straw decomposition and biochar disintegration with fresh straw on soil aggregation were minor and thus were neglected because the maximum impact of these factors on soil macro-aggregates occurs within the first 30 days (De Gryze et al. 2006; Zimmerman et al. 2011; Awad et al. 2013; Soinnie et al. 2014). (2) Biochar can increase soil water content, improve microbial activity, promote crosslinking of organic matter, and enhance the formation of aggregates (Abiven et al. 2008; Awad et al. 2013). However, in this study, the sampling time was during the late maize season, immediately after the end of the rainy season, and the biochar had little effect on soil moisture, which was difficult to observe because of the recent end of the rainy season. However, biochar can significantly improve the water content of surface soil during the winter wheat season (Liang et al. 2014). (3) The soil in this study was located in a continental monsoon climate zone which experiences significant freeze–thaw cycles. Thus, the freeze–thaw cycles are very destructive to soil aggregates (Staricka and Benoit 1995) and macro-aggregates in light soil with high moisture content (Six et al. 2004). Therefore, under our experimental conditions, the effect of biochar on soil aggregation was not significant.

The current literature is limited on the effects of soil carbonate on soil aggregation, and the overall results remain inconclusive. For example, some research has reported a significant positive correlation between soil carbonate content and soil aggregate stability (Mbagwu

and Bazzoffi 1998; Vaezi et al. 2008), whereas other research on a similar soil reported a positive correlation between higher carbonate content and the more unstable soil aggregates (Dimoyiannis 2012). Another study found that higher carbonate content in silt and clay makes soil aggregates unstable and the soil is thus more susceptible to erosion (Merzouk and Blake 1991). Research into SOC has shown that the formation of macro-aggregates was mainly dependent on carbonate content (Boix-Fayos et al. 2001). Soil in this study contained 17.3 g kg^{-1} of carbonate and was classified as mild calcareous soil. Because of space limitation, further work was not carried out on soil carbonates in this study, but this topic requires further study in the future.

4.2 Effects of biochar on the contents of organic carbon and total nitrogen in soil aggregates

Biochar application increased the total organic carbon and total nitrogen in the soil (Table 4), which was consistent with the research conducted by Liu et al. (2014). Because this research was based on wheat–maize rotation and straw return, the application of biochar boosted soil microbial activity (Steiner et al. 2008) and improved crop yields (Liu et al. 2014). This further promoted degradation and transformation of plant residues and increased SOC and total nitrogen amounts, which both showed a positive correlation with biochar dosages (Fig. 7).

Macro-aggregates are formed by micro-aggregates through organic adhesion (Tisdall and Oades 1982). Application of biochar can increase the soil CEC and water-holding ability, improve the quality of soil, and increase soil organic matter contents (Schmidt and Noack 2000; Lehmann et al. 2006). Biochar application also creates organic matter and micro-aggregates form macro-aggregates (Tisdall and Oades 1982). Six et al. (2002) found that SOC usually exists in macro-aggregates in the short term and then become small aggregates after an extended amount of time. Application of biochar in this study mainly improved the SOC and total nitrogen content of macro-aggregates, which was significantly correlated with the amount of biochar application (Fig. 7). Our results supported the prior findings of Zhang et al. (2015) and Liu et al. (2014).

Biochar mainly affects organic carbon and total nitrogen contents in the $>250\text{-}\mu\text{m}$ aggregates of light fractions and the $>1000\text{-}\mu\text{m}$ aggregates of heavy fractions. The organic carbon and total nitrogen were significantly increased with the increased amount of biochar added (Fig. 7). Organic carbon in soil light fractions mainly consists of animal and plant residues, mycelium, spores, monosaccharides, polysaccharides, and hemilignin (Christensen 2001). All these substances were found in macro-aggregates (Six et al. 2002). Therefore, the

concentration of organic carbon in light fractions was macro-aggregates, while the organic carbon in heavy fractions mainly existed as organic–inorganic complexes, which were mostly humus (Christensen 1992). Wu et al. (2004) reported that the turnover rate of light-fraction organic carbon was faster, at 2–11 times higher than that of the heavy fractions; thus, the heavy fractions are more sensitive to agricultural practices. Biochar enhances soil organic matter by altering the soil microenvironment (Schmidt and Noack 2000; Lehmann et al. 2006). This research supports the hypothesis that biochar mainly increases the SOC and total nitrogen contents in light fractions.

4.3 Effects of biochar on organic carbon properties in water-stable aggregates

Different functional groups have different absorption bands in FTIR analysis (Barje et al. 2012; El Fels et al. 2014). Figure 1 shows the FTIR spectra of the biochar used in this study, which only includes three main peaks: 1435 , 1038 , and 874 cm^{-1} attributed to carbonate, stretching of Si–O, and out-of-plane bending of the aromatic ring C–H bonds, respectively. It indicates that biochar has very little organic carbon and it also could be proved from Fig. 2, because except for the large amount of CO_2 , only very little (less than 0.5 %) benzene exists. Keiluweit et al. (2010) found biochar produced at high temperature would diminish its carbon functionalities and be transformed to graphite. So it indicated that biochar spectra would not affect soil organic spectra directly. The peaks obtained in this study were consistent with those of Calderón et al. (2013) and Peltre et al. (2014). The absorption peaks of organic carbon were observed at 3402 cm^{-1} and were found in all treatment groups of both light and heavy fractions, which indicates the presence of hydroxyl groups. However, peak frequencies in different treatments were inconsistent and were related to the aggregate sizes. The decrease in intensity of hydroxyl peaks between different treatments correlates with decreased aggregate diameter. In the $>1000\text{-}\mu\text{m}$ aggregates, the biochar-treated aggregates had the smallest peak, which can be explained by the hydroxyl and hydrogen bonding (El Fels et al. 2014). Higher content of biochar CEC (Downie et al. 2009; Chintala et al. 2014b) made the hydroxyl and hydrogen bonding more likely to occur. The 2922 cm^{-1} peak represents aliphatic C–H, which was found to be present in the light fractions and absent in the heavy fractions. Zhong et al. (2013) found that the FTIR spectrum of wheat straw contained methylene, which indicated that heavy fractions do not have unstable organics such as straw residue. Conversely, there was no observable methylene peak after biochar application in the $>1000\text{-}\mu\text{m}$ aggregates. Thus, it can be concluded that macro-aggregates are unstable and may transform methylene into other functional groups relatively rapidly. In addition, biochar can promote the transformation of organic carbon in macro-

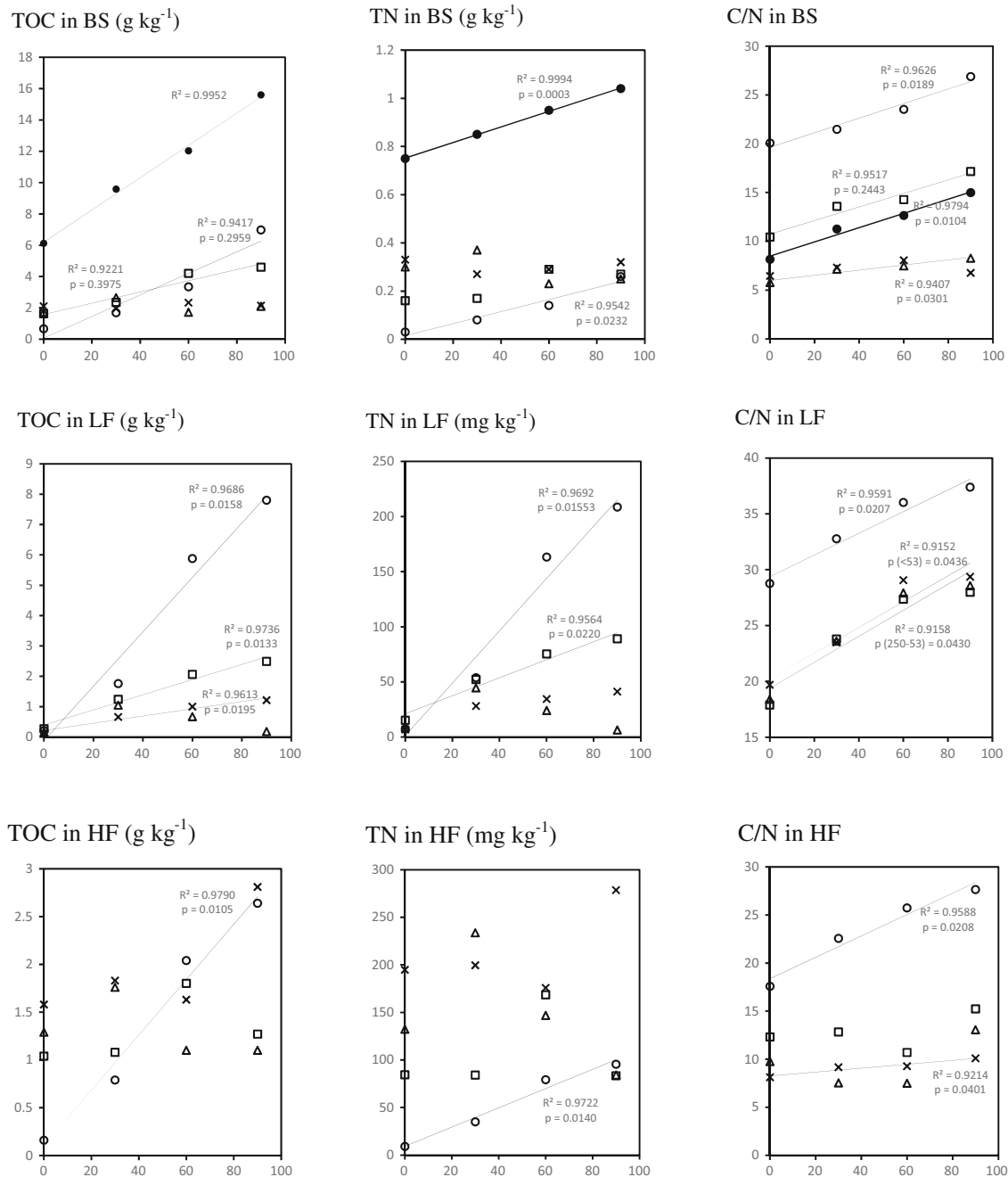


Fig. 7 Relationship between biochar amounts and *TOC*, *TN*, and *C/N*. Note: Closed circles, open circles, open squares, open triangles, and multiplication signs mean bulk soil and >1000-, 1000–250-, 250–53-, and <53- μm aggregates, respectively. The lines in each coordinate system stand for significant correlation ($p < 0.05$) between biochar

amounts (t ha^{-1}) and measured items. *BS* means bulk soil, *LF* means light fraction, and *HF* means heavy fraction in the aggregates. *TOC*, *TN*, and *C/N* refer to total organic carbon, total nitrogen, and the ratio of total organic carbon to total nitrogen, respectively

aggregates. The 1630 cm^{-1} peak represents aromatic C=C double bonds. Similarly to hydroxyl groups, only those treated by biochar had a reduced peak intensity. Since C=C double bonds are the product of aromatic rings containing lignin depolymerization and dehydrogenation (Lange 2007), it can be inferred that biochar application can improve the stability of

organic carbon. In the $1430\text{--}1440\text{ cm}^{-1}$ spectrum, biochar application resulted in asymmetrical deformation vibrations of methyl groups in the light-fraction organic carbon, which was observed within all sizes of aggregates. The 1384 cm^{-1} peak belongs to methyl groups, which supports the existence of fatty acids and polysaccharides with a low degree of

humification (Kalbitz et al. 1999). All the light fractions contained methyl, while in heavy fractions only the biochar-treated >1000- μm aggregates contained methyl, also indicating instability of the >1000- μm aggregates.

Using Py–GC–MS technology, complex pyrolysis products can be classified to distinguish different organic matter and determine their changes (Almendros et al. 1997). In this study, excluding CO_2 , the four main components were from alkane olefins, polysaccharides, lignins, and aromatic compounds, which together accounted for more than 80 % of the soil organic carbon pyrolysis across all sizes of aggregates. The pyrolysis products obtained in this study were consistent with those of De la Rosa et al. (2012). Alkane olefins and aromatic compounds are generally stable and do not easily decompose (Nierop 1998). Aromatic compounds usually exist in biochar or recombined organic compounds produced from incomplete combustion (Tinoco et al. 2006; Chintala et al. 2014c). Phenols and phenolic substances are usually products of lignin pyrolysis or demethylation from biodegradation of lignin (Sáiz-Jiménez and De Leeuw 1986). Polysaccharides are common organic compounds found in plants and soil organic matter and are vulnerable to heat transformation or biodegradation (Templier et al. 2005). CO_2 is cracked from active chemicals, and thus, it is difficult to determine its origin (Vancampenhout et al. 2009; Kaal et al. 2015). The Py–GC/MS result is consistent with the result of TOC and FTIR that biochar influences the light fraction of aggregates more than the heavy fraction and the effect decreased as the aggregate size decreased. In all sizes of aggregates from light fractions with biochar application, CO_2 is greater than the initial and B0 and has a decreasing trend when the diameter of aggregates decreases, which indicated that biochar increased the active chemical content in soil aggregates, but they cannot be identified using Py–GC/MS, because they were pyrolyzed into CO_2 directly. It could be explained using the result of biochar Py–GC/MS (Fig. 2) that the main pyrolysis product is CO_2 . Since the early stages of aggregate formation require unstable organic carbon (Six et al. 2004), it can be inferred that biochar increased the proportion of unstable organic carbon and promoted the formation of aggregates.

5 Conclusions

One-time applications of different amounts of biochar in calcareous soil had no noticeable significant impact on soil aggregation after 3 years but can reduce the breakage of soil macro-aggregates. Moreover, biochar significantly increased the TOC and TN contents as well as their ratios in soil macro-aggregates, improved the proportion of active components in

soil organic matter, and thus enhanced the protection of soil organic carbon by soil aggregates.

Under field conditions, the effects of biochar on soil aggregation were influenced by many factors. The evaluation results should be analyzed comprehensively with consideration of environmental factors and time effects. For seasonal parameters, the short-term effects of biochar application should be tracked. For calcareous soils, studies should focus on the impact of biochar on the soil carbonate progress.

Acknowledgments This work was supported by the National Natural Science Foundation of China (No. 41171211). We also thank Prof. Phil Brookes from Rothamsted Research, UK, for the great help in English writing during his visit to China Agricultural University.

References

- Abiven S, Menasseri S, Angers DA, Leterme P (2008) A model to predict soil aggregate stability dynamics following organic residue incorporation under field conditions. *Soil Sci Soc Am J* 72:119–125
- Abiven S, Menasseri S, Chenu C (2009) The effects of organic inputs over time on soil aggregate stability—a literature analysis. *Soil Biol Biochem* 41:1–12
- Almendros G, Dorado J, González-Vila FJ, Martín F (1997) Pyrolysis of carbohydrate-derived macromolecules: its potential in monitoring the carbohydrate signature of geopolymers. *J Anal Appl Pyrolysis* 40:599–610
- Angers D, Samson N, Legere A (1993) Early changes in water-stable aggregation induced by rotation and tillage in a soil under barley production. *Can J Soil Sci* 73:51–59
- Awad Y, Blagodatskaya E, Ok Y, Kuzyakov Y (2013) Effects of polyacrylamide, biopolymer and biochar on the decomposition of ^{14}C -labelled maize residues and on their stabilization in soil aggregates. *Eur J Soil Sci* 64:488–499
- Barje F, El Fels L, El Hajjoui H, Amir S, Winterton P, Hafidi M (2012) Molecular behaviour of humic acid-like substances during co-composting of olive mill waste and the organic part of municipal solid waste. *Int Biodeterior Biodegrad* 74:17–23
- Boix-Fayos C, Calvo-Cases A, Imeson A, Soriano-Soto M (2001) Influence of soil properties on the aggregation of some Mediterranean soils and the use of aggregate size and stability as land degradation indicators. *Catena* 44:47–67
- Brodowski S, John B, Flessa H, Amelung W (2006) Aggregate-occluded black carbon in soil. *Eur J Soil Sci* 57:539–546
- Bronick CJ, Lal R (2005) Soil structure and management: a review. *Geoderma* 124:3–22
- Bühmann C, Beukes D, Turner D (2006) Clay mineral associations in soils of the Lusikisiki area, Eastern Cape Province, and their agricultural significance. *S Afr J Plant Soil* 23:78–86
- Calderón F, Haddix M, Conant R, Magrini-Bair K, Paul E (2013) Diffuse-reflectance fourier-transform mid-infrared spectroscopy as a method of characterizing changes in soil organic matter. *Soil Sci Soc Am J* 77:1591–1600
- Carr AS, Boom A, Chase BM, Meadows ME, Roberts ZE, Britton MN, Cumming AMJ (2013) Biome-scale characterisation and differentiation of semi-arid and arid zone soil organic matter compositions using pyrolysis–GC/MS analysis. *Geoderma* 200–201:189–201
- Chintala R, Mollinedo J, Schumacher TE, Malo DD, Julson JL (2014a) Effect of biochar on chemical properties of acidic soil. *Arch Agron Soil Sci* 60:393–404

- Chintala R, Schumacher TE, Kumar S, Malo DD, Rice JA, Bleakley B, Chilom G, Clay DE, Julson JL, Papiernik SK, Gu ZR (2014b) Molecular characterization of biochars and their influence on microbiological properties of soil. *J Hazard Mater* 279:244–256
- Chintala R, Schumacher TE, McDonald LM, Clay DE, Malo DD, Papiernik SK, Clay SA, Julson JL (2014c) Phosphorus sorption and availability from biochars and soil/biochar mixtures. *CLEAN: Soil Air Water* 42:626–634
- Chivenge P, Vanlauwe B, Gentile R, Six J (2011) Organic resource quality influences short-term aggregate dynamics and soil organic carbon and nitrogen accumulation. *Soil Biol Biochem* 43:657–666
- Christensen BT (1992) Physical fractionation of soil and organic matter in primary particle size and density separates. In: Stewart BA (ed) *Advances in soil science*. Springer, New York, pp 1–90
- Christensen BT (2001) Physical fractionation of soil and structural and functional complexity in organic matter turnover. *Eur J Soil Sci* 52: 345–353
- Dalal R, Bridge B (1996) Aggregation and organic matter storage in sub-humid and semi-arid soils. Structure and organic matter storage in agricultural soils. CRC/Lewis Publishers, Boca Raton
- De Gryze S, Six J, Merckx R (2006) Quantifying water-stable soil aggregate turnover and its implication for soil organic matter dynamics in a model study. *Eur J Soil Sci* 57:693–707
- De la Rosa JM, Faria SR, Varela ME, Knicker H, González-Vila FJ, González-Pérez JA, Keizer J (2012) Characterization of wildfire effects on soil organic matter using analytical pyrolysis. *Geoderma* 191:24–30
- Denef K, Six J, Merckx R, Paustian K (2002) Short-term effects of biological and physical forces on aggregate formation in soils with different clay mineralogy. *Plant Soil* 246:185–200
- Dimoyiannis D (2012) Wet aggregate stability as affected by excess carbonate and other soil properties. *Land Degrad Dev* 23:450–455
- Downie A, Crosky A, Munroe P (2009) Physical properties of biochar. *Biochar for environmental management: science and technology* 13–32
- El Fels L, Zamama M, El Asli A, Hafidi M (2014) Assessment of bio-transformation of organic matter during co-composting of sewage sludge-lignocellulosic waste by chemical, FTIR analyses, and phytotoxicity tests. *Int Biodeterior Biodegrad* 87:128–137
- Ellerbrock RH, Gerke HH (2004) Characterizing organic matter of soil aggregate coatings and biopores by Fourier transform infrared spectroscopy. *Eur J Soil Sci* 55:219–228
- Elliott E (1986) Aggregate structure and carbon, nitrogen, and phosphorus in native and cultivated soils. *Soil Sci Soc Am J* 50:627–633
- Fonte SJ, Yeboah E, Ofori P, Quansah GW, Vanlauwe B, Six J (2009) Fertilizer and residue quality effects on organic matter stabilization in soil aggregates. *Soil Sci Soc Am J* 73:961–966
- Golchin A, Oades J, Skjemstad J, Clarke P (1994) Study of free and occluded particulate organic matter in soils by solid state ¹³C CP/MAS NMR spectroscopy and scanning electron microscopy. *Soil Res* 32:285–309
- Guto S, Pypers P, Vanlauwe B, de Ridder N, Giller KE (2011) Tillage and vegetative barrier effects on soil conservation and short-term economic benefits in the Central Kenya highlands. *Field Crop Res* 122:85–94
- Hardie M, Clothier B, Bound S, Oliver G, Close D (2014) Does biochar influence soil physical properties and soil water availability? *Plant Soil* 376:347–361
- Jastrow J, Miller R, Lussenhop J (1998) Contributions of interacting biological mechanisms to soil aggregate stabilization in restored prairie. *Soil Biol Biochem* 30:905–916
- Jeffery S, Meinders MB, Stoof CR, Bezemer TM, van de Voorde TF, Mommer L, van Groenigen JW (2015) Biochar application does not improve the soil hydrological function of a sandy soil. *Geoderma* 251:47–54
- Jien S-H, Wang C-S (2013) Effects of biochar on soil properties and erosion potential in a highly weathered soil. *Catena* 110:225–233
- Kaal J, Cortizas AM, Rydberg J, Bigler C (2015) Seasonal changes in molecular composition of organic matter in lake sediment trap material from Nylandssjön, Sweden. *Org Geochem* 83:253–262
- Kalbitz K, Geyer W, Geyer S (1999) Spectroscopic properties of dissolved humic substances—a reflection of land use history in a fen area. *Biogeochemistry* 47:219–238
- Kay B (1998) Soil structure and organic carbon: a review. *Soil processes and the carbon cycle* 169–197
- Keiluweit M, Nico PS, Johnson MG, Kleber M (2010) Dynamic molecular structure of plant biomass-derived black carbon (biochar). *Environ Sci Technol* 44:1247–1253
- Lado M, Ben-Hur M, Shainberg I (2004) Soil wetting and texture effects on aggregate stability, seal formation, and erosion. *Soil Sci Soc Am J* 68:1992–1999
- Laird DA, Brown RC, Amonette JE, Lehmann J (2009) Review of the pyrolysis platform for coproducing bio-oil and biochar. *Biofuels Bioprod Biorefin* 3:547–562
- Lange JP (2007) Lignocellulose conversion: an introduction to chemistry, process and economics. *Biofuels Bioprod Biorefin* 1:39–48
- Le Bissonnais Y (1996) Aggregate stability and assessment of soil crustability and erodibility: I. theory and methodology. *Eur J Soil Sci* 47:425–437
- Lehmann J, Gaunt J, Rondon M (2006) Bio-char sequestration in terrestrial ecosystems—a review. *Mitig Adapt Strateg Glob Chang* 11: 395–419
- Lehrsch G, Sojka R, Carter D, Jolley P (1991) Freezing effects on aggregate stability affected by texture, mineralogy, and organic matter. *Soil Sci Soc Am J* 55:1401–1406
- Liang F, Li G-T, Lin Q-M, Zhao X-R (2014) Crop yield and soil properties in the first 3 years after biochar application to a calcareous soil. *J Integr Agric* 13:525–532
- Lin Y, Munroe P, Joseph S, Kimber S, Van Zwieten L (2012) Nanoscale organo-mineral reactions of biochars in ferrosol: an investigation using microscopy. *Plant Soil* 357:369–380
- Liu X-H, Han F-P, Zhang X-C (2012) Effect of biochar on soil aggregates in the Loess Plateau: results from incubation experiments. *Int J Agric Biol* 14:975–979
- Liu Z, Chen X, Jing Y, Li Q, Zhang J, Huang Q (2014) Effects of biochar amendment on rapeseed and sweet potato yields and water stable aggregate in upland red soil. *Catena* 123:45–51
- Lu R-K (2000) *Methods of soil and agrochemical analysis*. China Agricultural Science and Technology Press, Beijing (in Chinese)
- Lu S-G, Sun F-F, Zong Y-T (2014) Effect of rice husk biochar and coal fly ash on some physical properties of expansive clayey soil (Vertisol). *Catena* 114:37–44
- Luo Y, Durenkamp M, De Nobili M, Lin Q, Brookes PC (2011) Short term soil priming effects and the mineralisation of biochar following its incorporation to soils of different pH. *Soil Biol Biochem* 43:2304–2314
- Mbagwu J, Bazzoffi P (1998) Soil characteristics related to resistance of breakdown of dry soil aggregates by water-drops. *Soil Tillage Res* 45:133–145
- Merzouk A, Blake G (1991) Indices for the estimation of interrill erodibility of Moroccan soils. *Catena* 18:537–550
- Mollinedo J, Schumacher TE, Chintala R (2015) Influence of feedstocks and pyrolysis on biochar's capacity to modify soil water retention characteristics. *J Anal Appl Pyrolysis* 114:100–108
- Nierop K (1998) Origin of aliphatic compounds in a forest soil. *Org Geochem* 29:1009–1016
- Oades J (1993) The role of biology in the formation, stabilization and degradation of soil structure. *Geoderma* 56:377–400
- Oades J, Waters A (1991) Aggregate hierarchy in soils. *Soil Res* 29:815–828

- Ojeda G, Mattana S, Àvila A, Alcañiz JM, Volkmann M, Bachmann J (2015) Are soil–water functions affected by biochar application? *Geoderma* 249:1–11
- Peake LR, Reid BJ, Tang X (2014) Quantifying the influence of biochar on the physical and hydrological properties of dissimilar soils. *Geoderma* 235:182–190
- Pedersen JA, Simpson MA, Bockheim JG, Kumar K (2011) Characterization of soil organic carbon in drained thaw-lake basins of Arctic Alaska using NMR and FTIR photoacoustic spectroscopy. *Org Geochem* 42:947–954
- Peltre C, Bruun S, Du C, Thomsen IK, Jensen LS (2014) Assessing soil constituents and labile soil organic carbon by mid-infrared photoacoustic spectroscopy. *Soil Biol Biochem* 77:41–50
- Plaza-Bonilla D, Álvaro-Fuentes J, Cantero-Martínez C (2013) Soil aggregate stability as affected by fertilization type under semiarid no-tillage conditions. *Soil Sci Soc Am J* 77:284–292
- Polak J, Sułkowski W, Bartoszek M, Luty A, Pentak D, Sułkowska A (2007) Spectroscopic study of the effect of biological treatment on the humification process of sewage sludge. *J Mol Struct* 834: 229–235
- Rhoades JD (1986) Cation exchange capacity. In: Page AL, Miller RH, Keeney DR (eds) *Methods of soil analysis. Part 2. Chemical and microbiological properties*, 2nd edn. ASA and SSSA, Madison, pp 149–157, **Agronomy Monograph No. 9**
- Rossel RAV, Behrens T (2010) Using data mining to model and interpret soil diffuse reflectance spectra. *Geoderma* 158:46–54
- Sáiz-Jiménez C, De Leeuw J (1986) Chemical characterization of soil organic matter fractions by analytical pyrolysis–gas chromatography–mass spectrometry. *J Anal Appl Pyrolysis* 9:99–119
- Schmidt MW, Noack AG (2000) Black carbon in soils and sediments: analysis, distribution, implications, and current challenges. *Glob Biogeochem Cycles* 14:777–793
- Simkovic I, Dlapa P, Doerr SH, Mataix-Solera J, Sasinkova V (2008) Thermal destruction of soil water repellency and associated changes to soil organic matter as observed by FTIR spectroscopy. *Catena* 74: 205–211
- Six J, Paustian K, Elliott E, Combrink C (2000) Soil structure and organic matter I. distribution of aggregate-size classes and aggregate-associated carbon. *Soil Sci Soc Am J* 64:681–689
- Six J, Conant RT, Paul EA, Paustian K (2002) Stabilization mechanisms of soil organic matter: implications for C-saturation of soils. *Plant Soil* 241:155–176
- Six J, Bossuyt H, Degryze S, Denef K (2004) A history of research on the link between (micro) aggregates, soil biota, and soil organic matter dynamics. *Soil Tillage Res* 79:7–31
- Smidt E, Meissl K (2007) The applicability of fourier transform infrared (FT-IR) spectroscopy in waste management. *Waste Manage* 27:268–276
- Soinne H, Hovi J, Tammeorg P, Turtola E (2014) Effect of biochar on phosphorus sorption and clay soil aggregate stability. *Geoderma* 219:162–167
- Soriano-Disla JM, Janik LJ, Viscarra Rossel RA, Macdonald LM, McLaughlin MJ (2014) The performance of visible, near-, and mid-infrared reflectance spectroscopy for prediction of soil physical, chemical, and biological properties. *Appl Spectrosc Rev* 49: 139–186
- Staricka J, Benoit G (1995) Freeze-drying effects on wet and dry soil aggregate stability. *Soil Sci Soc Am J* 59:218–223
- Steiner C, Das KC, Garcia M, Förster B, Zech W (2008) Charcoal and smoke extract stimulate the soil microbial community in a highly weathered xanthic Ferralsol. *Pedobiologia* 51:359–366
- Stemmer M, Gerzabek MH, Kandeler E (1998) Organic matter and enzyme activity in particle-size fractions of soils obtained after low-energy sonication. *Soil Biol Biochem* 30:9–17
- Templier J, Derenne S, Croué J-P, Largeau C (2005) Comparative study of two fractions of riverine dissolved organic matter using various analytical pyrolytic methods and a ¹³C CP/MAS NMR approach. *Org Geochem* 36:1418–1442
- Tinoco P, Almendros G, Sanz J, González-Vázquez R, González-Vila FJ (2006) Molecular descriptors of the effect of fire on soils under pine forest in two continental Mediterranean soils. *Org Geochem* 37: 1995–2018
- Tisdall J, Oades JM (1982) Organic matter and water-stable aggregates in soils. *J Soil Sci* 33:141–163
- Vaezi A, Sadeghi S, Bahrami H, Mahdian M (2008) Modeling the USLE K-factor for calcareous soils in northwestern Iran. *Geomorphology* 97:414–423
- Vancampenhout K, Wouters K, De Vos B, Buurman P, Swennen R, Deckers J (2009) Differences in chemical composition of soil organic matter in natural ecosystems from different climatic regions—a pyrolysis–GC/MS study. *Soil Biol Biochem* 41:568–579
- White DM, Hodgkinson ID, Seelen SJ, Coulson SJ (2007) Characterization of soil carbon from a Svalbard glacier-retreat chronosequence using pyrolysis–GC/MS analysis. *J Anal Appl Pyrolysis* 78:70–75
- Wu T-Y, Jeff JS, Li F-M, Qian P-Y, Zhang S-Q, Sukhadev SM, Wang F (2004) Concepts and relative analytical techniques of soil organic matter. *Chin J Appl Ecol* 15:717–722 (in Chinese)
- Zelazny LW, He L, Vanwormhoudt AM (1996) Charge analyses of soils and anion exchange. In: Sparks DL (ed) *Methods of soil analysis, part 3: chemical methods*. Soil Science Society of America, Madison, SSSA Book Series no. 5
- Zhang H, Voroney R, Price G (2015) Effects of temperature and processing conditions on biochar chemical properties and their influence on soil C and N transformations. *Soil Biol Biochem* 83:19–28
- Zhong C, Wang C, Huang F, Jia H, Wei P (2013) Wheat straw cellulose dissolution and isolation by tetra-n-butylammonium hydroxide. *Carbohydr Polym* 94:38–45
- Zimmerman AR, Gao B, Ahn M-Y (2011) Positive and negative carbon mineralization priming effects among a variety of biochar-amended soils. *Soil Biol Biochem* 43:1169–1179